HYDRAULIC FRACTURING EFFECTIVENESS ASSESMENT IN TIGHT RESERVOIRS AND MAIN CONSIDERATIONS FOR TREATMENT DESIGN AND PLANNING: Case Study, Austral Basin, Argentina

Miguel Jardel, Halliburton, miguel.jardel@halliburton.com; Santiago Casala, Halliburton, santiago.casala@halliburton.com;
Maria Florencia Melendo, CGC, florencia.melendo@cgc.com.ar; Gustavo Kruse, Consultant, kgrust@hotmail.com.

Key words

Fracture growth assessment, hydraulic stimulation, Campo Indio, Cuenca Austral, Tight

Summary

El reciente interés que han adquirido los recursos no convencionales en Argentina, promovido por incentivos y recortes de impuestos, han atraído a empresas de petróleo y gas de vuelta a la Cuenca Austral situada al sur de Argentina. Varios campos fueron abandonados en el pasado; sin embargo, recientemente, a través de tratamientos de estimulación hidráulica más efectivos, algunos campos fueron recuperados exhibiendo tasas de producción significativas.

El caso de estudio presentado en este trabajo muestra el rápido aumento en la producción de gas del miembro tight M1 de la formación Magallanes, a través de la estimulación por fracturamiento hidráulico. Sin embargo, se plantearon interrogantes al evaluar la efectividad de los tratamientos de fractura encontrando que la altura de fractura se había extendido más allá de los límites del reservorio productivo, resultando en un gasto adicional de propante. En consecuencia, el optimizar los tratamientos de fractura hidráulica adquirió alta prioridad porque es la estrategia primaria para alcanzar el volumen ideal de reservorio estimulado.

Este documento describe los resultados obtenidos en dos pozos donde fue utilizado propante no radiactivo trazable para evaluar la altura de fractura después del tratamiento de estimulación hidráulica, para proporcionar información sobre la geometría de la fractura y su extensión vertical. La evaluación de altura de fractura observada en los pozos, proporcionó resultados diferentes a pesar de tratarse de la misma formación con propiedades de roca muy similares.

La revisión realizada mediante el procesamiento de perfiles y la simulación de las fracturas realizadas, permitió determinar las variables que afectan el comportamiento del crecimiento de fractura, como ser el contraste de estrés, las propiedades petrofísicas y de la roca y las condiciones de la cementación, entre otras.

Abstract

The recent interest that unconventional resources has gained in Argentina, promoted by tax cut incentives, has attracted oil and gas companies back to the Austral basin of southern Argentina. Several fields were abandoned in the past; however, recently, through more effective hydraulic stimulation treatments, some fields were "brought back to life," exhibiting meaningful production rates.

The case study presented in this paper shows the rapid increase in gas rate production from the tight M1 member of the Magallanes formation through hydraulic fracturing stimulation. However, issues arose when evaluating the effectiveness of the fracture treatments and finding that the fracture height had extended beyond the boundaries of the productive reservoir, and resulting in a waste of proppant. Consequently, optimizing hydraulic fracture treatments became a high priority because it is the primary strategy for achieving the ideal stimulated reservoir volume (SRV).

This paper describes the results obtained in two wells in which traceable non-radioactive proppant was used to assess the fracture height after hydraulic stimulation treatment to obtain information about the fracture geometry and vertical extension. The fracture height assessment observed in these wells provided different results, despite treating the same formation with very similar rock properties. The formation assessment made by log processing and fracture simulations helped to evaluate variables that affect fracture growth behavior, such as stress contrast, rock and petrophysical properties, and cementing conditions.

Introduction

Hydraulic fracture (HF) stimulation treatments have evolved over the years in terms of job magnitude, increased number of stages in each well, and increased amount of pumped proppant; this evolution led to the modification of operating conditions and the need for certain resources. Consequently, those analyses led to new HF designs. This is the case of the evolution of the HF treatments performed in the Magallanes formation of Campo Indio field, more precisely in the productive "sand" called M1. The Campo Indio field is in the Austral basin, which is located in southern Argentina.

This document presents characteristics of the Austral basin, formations that compose it, location and characteristics of the reservoir rock of the Magallanes formation, and how it is constituted.

Reservoir properties that are essential for HF stimulation designs were defined from a geomechanical study and the analysis of well logs. This paper presents the HF stimulation programs defined for two assessed wells, the values obtained from simulations performed for each design, and the results obtained after the adjustments made for each operation. It also demonstrates how the final geometry of each treatment was evaluated, describes the factors that greatly affected the results, and presents the conclusions that were obtained to generate future designs of stimulation treatments.

Campo Indio Magallanes Field Location

The Campo Indio Magallanes field is located in the province of Santa Cruz, 140 km northwest of Río Gallegos (Fig. 1). The field covers an area of 76.29 km^2; to date, more than 70 wells have been drilled, of which 90% are currently producing gas and associated condensate.

The deposit toward the west of the field shows conventional characteristics; deposits on the east side of the field indicate characteristics of a tight deposit.

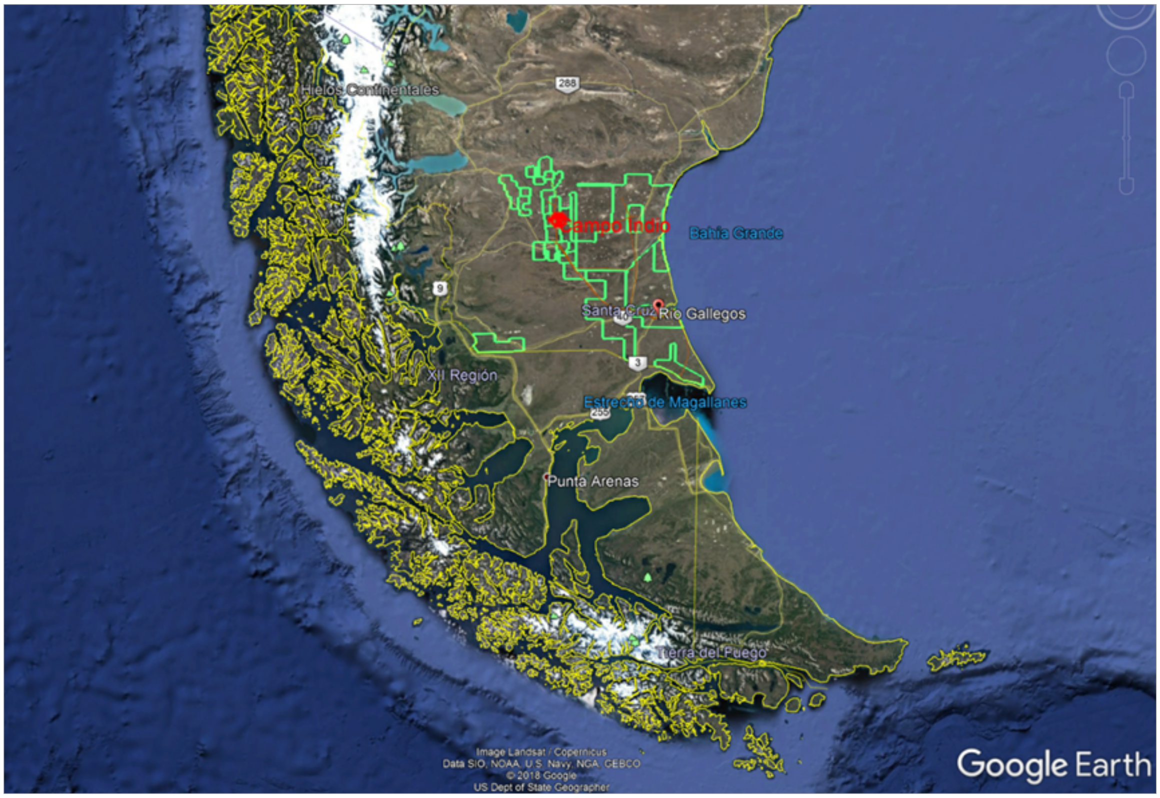

Fig. 1 – Campo Indio field location – Austral basin.

Geological Framework

The Austral basin is also known as the Magallanes basin. It is located on the southern tip of the South American continent, in the Argentine province of Santa Cruz, in the Chilean province of Magallanes, on the large island of Tierra del Fuego, and on an important surface of the Argentine Continental Platform. This basin covers a total area of 230,000 km^2, of which 85% is developed in the Argentine Republic.

The sedimentary column reaches a maximum thickness of 8000 m, with almost exclusive development of clastic rocks. The carbonate sediments only occur in some areas of the basin and have reduced thickness.

The Magallanes formation is subdivided into two members, of which the Lower Member presents the productive reservoirs. This member is of the Upper Cretaceous - Lower Tertiary age (Fig. 2).

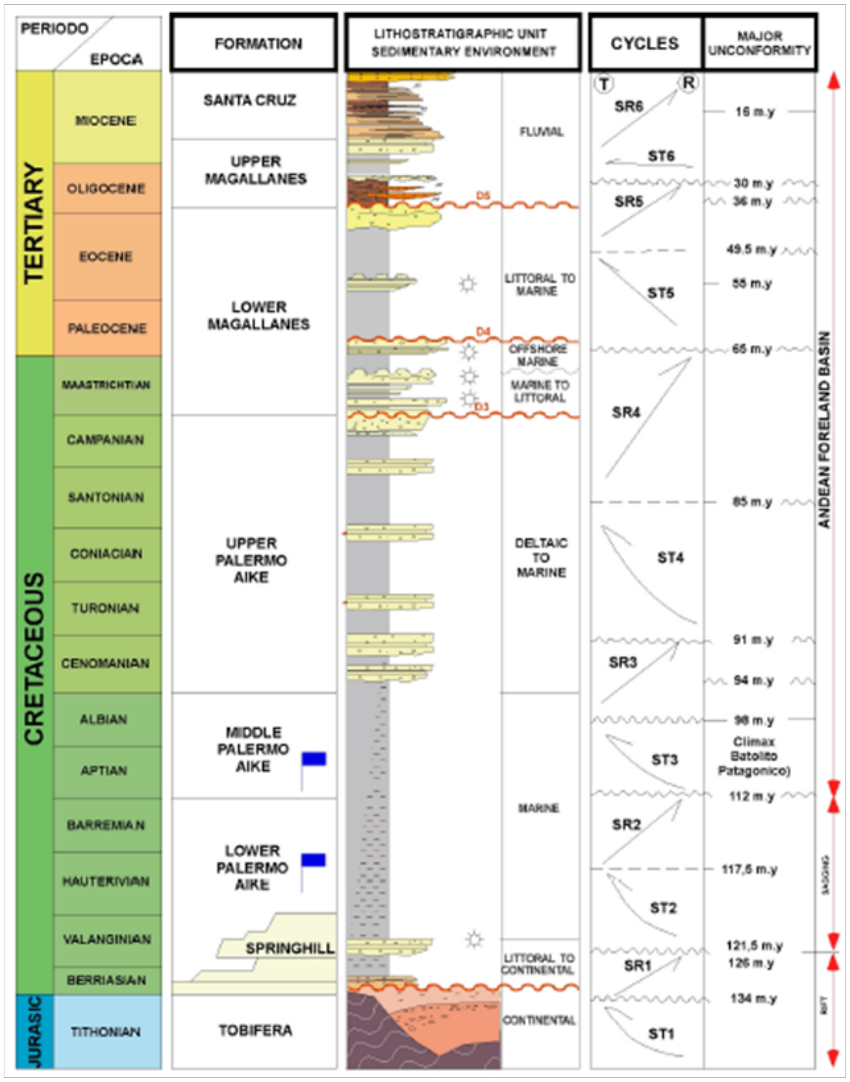

Fig. 2 – Stratigraphic column.

Structural Framework

The geological structure of the Campo Indio Magallanes field presents a homoclinal geometry. In this area, the post-Danian discordance is represented by the paleogeography generated from the tertiary reactivation of basement faults and the subsequent erosion. The original distribution of basement faults and their consequent reactivation generated two main depocenters separated by structural height. One of these depocenters has a north-south direction and belongs to the Boleadoras field. The second depocenter, with a main axis of northeast-southwest, is part of the Campo Indio field.

In general, faults have a negative flower feature. Some of the main faults (synthetic) have their roots in the Serie Tobífera formation or in the lower section of the Palermo Aike formation; these faults connect the source rock with the reservoirs and could have acted as migration routes.

The systems of extensional faults that affect the reservoir are secondary, generally of little geological relief, with a predominantly northwest-southeast orientation. Although they sometimes make up some accumulation limit, they do not play an important role (Fig. 3).

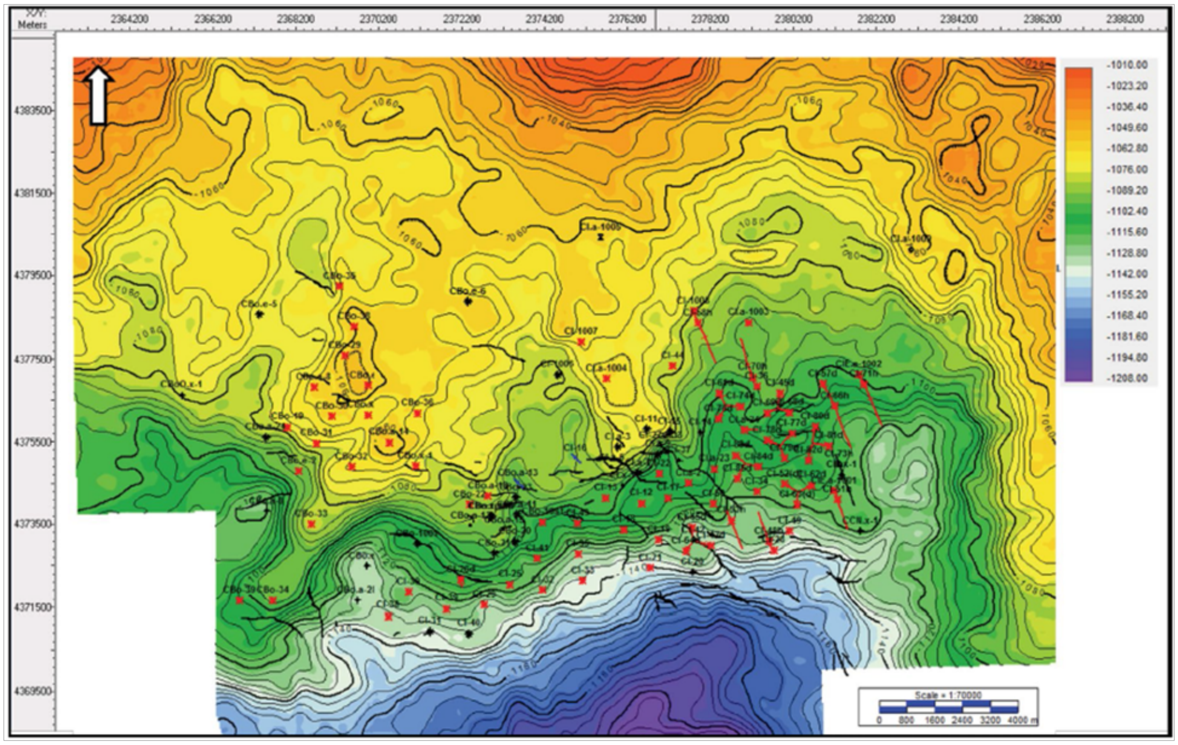

Fig. 3–Structural map in depth of post-Danian discordance (D4) that constitutes the M1 reservoir roof.

Stratigraphy

At the regional level, the lower member of the Magallanes formation is crossed by a regional discordance of an erosive nature (post-Danian discordance) that separates two tectonic sequences of the second order. The first tectonic sequence is of the Maastrichtian – Paleocene geological age and contains the sandstones M2 and M3. The second sequence is of the Paleocene - Middle Eocene geological age, and represents the post-tectonic sediments filling constituting the M1 sandstone.

The M1 sandstones are productive in the Campo Indio Magallanes field (Fig. 4).

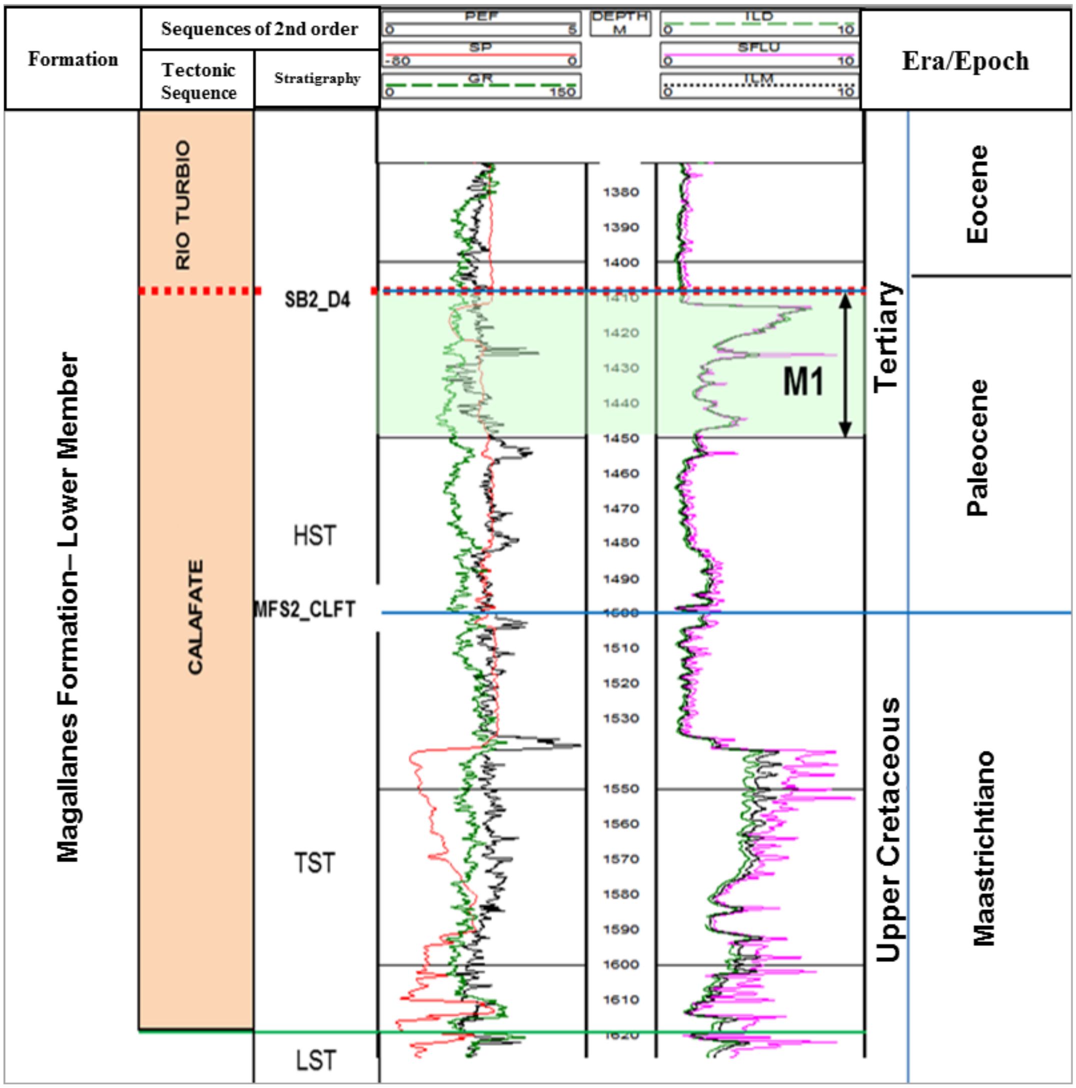

Fig. 4 – Chronostratigraphic column – sandstone M1.

Description of the MI Reservoir

Aimar et al. (2018) describe the M1 reservoir from the lithological point of view as fine to very fine sandstones of lithic-feldespathic and lithic composition.

The original pressure of the reservoir is approximately 2,000 psi, which corresponds to a depth of 1420.0 m.

The total productive interval of the sandy pack is approximately 25 m and the temperature is 170 °F. The porosity values range from approximately 15 to 35%. Laboratory data shows that permeability values vary laterally in the reservoir from 100 mD in the conventional facies to 0.1 to 1.0 mD in the tight facies.

Production History

During delineation and exploitation stages of the accumulation, a noticeable deterioration of the reservoir conditions toward the east was identified, which resulted in reservoirs of low permeability ("tight"), with traces of gas and surgent gas without pressure. During this stage, few holes were drilled, which were left with subcommercial, suspended, and abandoned productions.

As of 2015, CGC initiated the exploitation of the field, giving it a new approach. Goals associated with this exploitation included determining the geological limits of the field and defining the strategy and techniques that would enable commercial development of these tight reservoirs.

After a year of re-engineering the well model, the CGC completion team introduced two designs with the aim of achieving greater productivity through greater stimulation load and a reduction in the cost of well construction. These designs were documented by Solanet and Melendo (2017).

The first idea was to reduce the construction costs of wells through a monobore type well design, with the tubing cemented in front of the formation. A benefit of this new design includes the reduction of costs associated with excess materials used in the construction of a conventional well with a configuration of casing with tubing and packer; in addition, the HF would be "rig-less" because no tubing maneuvers are required. These monobore wells were arranged in a configuration of three-well clusters, departing from the same surface location (pad). This configuration reduced costs because less infrastructure is required, but the cost is increased because of the need to deviate the wells during perforation. The objective of the second idea was to increase well productivity by designing a horizontal well with multiple fractures.

The completion of the horizontal section consisted of a non-cemented liner, isolated by sleeves and packers. This design is more expensive than a conventional well in the area, but seeks to change the economic equation through an increase in production.

Conversely, to develop these areas, it was possible to fit them within a tight development as "Unconventional Exploitation Area – Campo Indio Eastern Field," being the first concession with a differential price outside of the Neuquina basin.

In 2017, a very intensive drilling campaign was performed in the area, which enabled the discovery of extensions to the north, doubling the exploitation area and sextupling the production of Campo Indio field. The production increased rapidly from 600 Mm^3/d in 2014 to 4252 Mm^3/d in November 2018, as shown in Fig. 5.

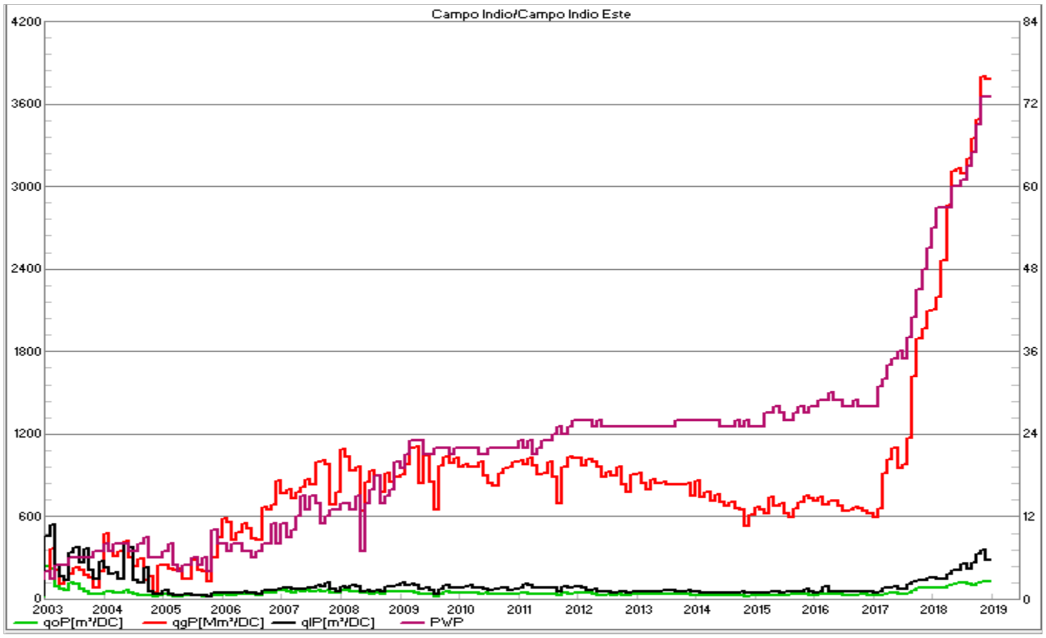

Fig. 5 – Production history and number of wells in production.

Background of Hydraulic Fractures

To date, there are more than 70 wells in which HF treatments were performed in the tight area of the Campo Indio field. The HF designs were initially oriented to ensure that the treatments performed provided a balance between a conservative program, with regard to the number of sacks of proppant pumped, and reasonable expenditures per stage. Based on the production response of the wells, more aggressive pumping schemes were sought to optimize the HF treatments.

Primary considerations to achieve these objectives include the following:

- Achieve the greatest possible conductive length (Xf) because the area does not have significant stress contrasts, and fractures would tend to grow in height. This idea is under evaluation because sufficient production data exists to begin the analysis. As part of this continuous improvement process, various optimization options were considered, such as fluid and propping agent types and other control parameters.
- Control the return of sand production. Various techniques and resources available in the market have been used to mitigate sand production, such as chemicals that act by agglutinating the grains of sand with sufficient resistance to withstand the pressure of flow, and curable resin sands that work at low confining pressures and in the temperature range of the Magallanes formation. As part of the control, a perforation process was adopted that uses 2-m sections perforated with high penetration charges and 2-in. perforating guns.
- Optimize the use and type of water as a critical resource. Although it was possible to use production water from a nearby well, this water is far from ideal for the correct operation of chemical additives. Several tests and laboratory calibrations must be performed for the field water samples, as well as simulations to replicate the conditions to which the fluid will be subjected throughout the process, from the preparation of the activated fluid (crosslinked) to the flowback.

Perforations

Progress was made in the wells by perforating 2 to 3 meter length intervals with two objectives: to reduce the return of proppant and to avoid the generation of multiple fractures. Because the creation of multiple fractures affects the final geometry obtained after a HF, the design of the perforation type is relevant from this aspect.

Guns used in most wells have been 2-in. diameter high shot density (HSD) perforations.

Fracture Design

To obtain the maximum economic return, fractures are optimized through various compositional and geometric parameters, such as the fracture length, amount, size and concentration of proppant, type of fluid, and the ratio of the pad volume with respect to the total volume pumped.

To define the number of sacks of proppant to be pumped in each HF, two types of studies were performed. First, conductive fracture length (Xf) sensitivities were simulated with respect to the proppant placed in formation (Fig. 6). In general terms, an incremental relationship was found to exist between the number of sacks of proppant pumped and production. Consequently, it was decided to perform fractures of greater dimensions, provided that the marginal increase in associated costs is offset by production increase.

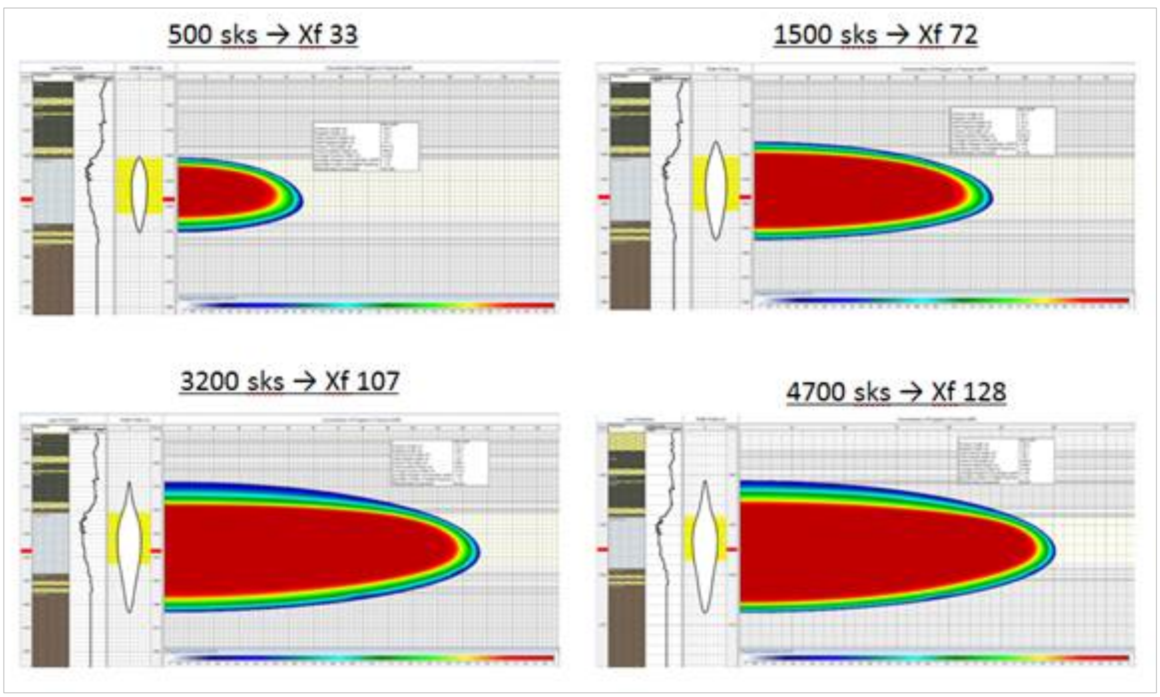

Fig. 6 – Fracture simulations: number of sacks vs. fracture length.

Second, the performance observed in past HF was studied. The ratio of sacks (100 lb) of proppant per meter of total M1 layer thickness (gross) was analyzed. As shown in Fig. 7, higher initial productions are obtained by increasing the ratio of sacks of proppant pumped per meter of M1 thickness. At the beginning of the development of the Campo Indio field, 20 sacks per meter of total thickness were pumped; currently, that quantity has increased to more than 120 sacks pumped per meter of M1 gross thickness.

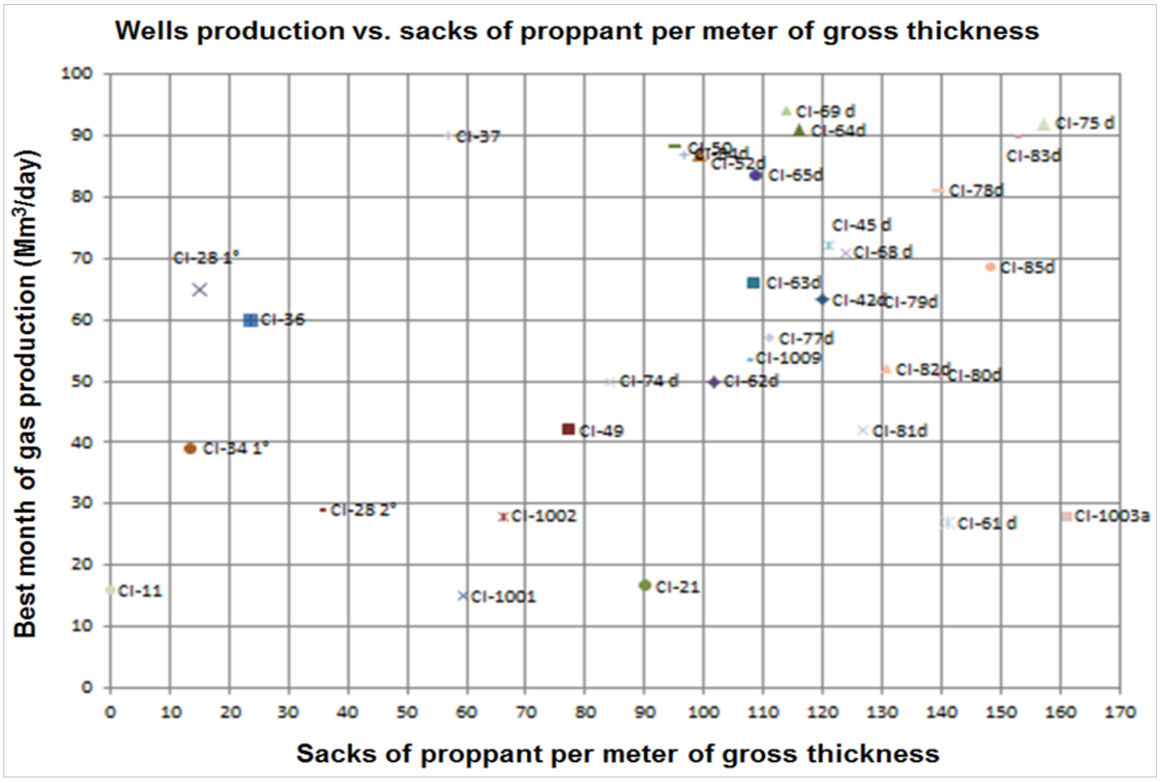

Fig. 7 – Wells production vs. sacks of proppant per meter of M1 gross thickness.

Diagnostic Pumping Analysis: DFIT and Minifrac

During the development of the field, multiple diagnostic pumping tests have been performed, such as the diagnostic fluid injection test (DFIT) and the mini-fracture (minifrac) types. The objective of the DFIT was to determine the closure pressure, and the permeability and reservoir pressures.

In the case of the minifrac, although closure formation pressure can be also assessed, the primary objective was to determine the perforation frictions and fluid efficiency. In this way, it is possible to determine whether or not it is necessary to modify the HF program by mixing some ceramic agent pill to erode perforations, or whether or not it is necessary to modify the pad volume proposed in the initial HF design.

Table 1 summarizes the parameters obtained from DFIT and minifrac diagnostic pumping tests. Types of leakoff include pressure dependent leakoff (PDL), high recession (HR), and normal leakoff (NL).

Table 1 - DFIT and Minifrac - Campo Indio Field								
Well	DFIT				Minifrac			
	Leakoff Type	Fracture Gradient	Closure Gradient	Pore Pressure Gradient	Leakoff Type	Fracture Gradient	Closure Gradient	Pore Pressure Gradient
		psi/ft	psi/ft	psi/ft		psi/ft	psi/ft	psi/ft
CI-34 1º						0.63		
CI-1001						0.63		
CI-1002						0.65		
CI-49	PDL		0.45	0.43	PDL	0.62		
CI-50	HR	0.56	0.52	0.41	HR	0.57	0.52	0.43
CI-21	NL	0.52	0.46	0.41	HR+NL	0.51	0.45	0.36
CI-52d					HR	0.59		
CI-62d					HR+NL	0.66		
CI-63d					PDL+HR	0.62		
CI-65d	PDL	0.56	0.52	0.46		0.57		
CI-1004a						0.64		
CI-61d		0.59				0.58		
CI-74d						0.56		
CI-75d						0.57		
CI-77d					HR	0.58	0.54	
CI-80d						0.59	0.53	
CI-87					HR+NL	0.56	0.52	
CI-88	HR	0.56	0.49	0.36	HR		0.50	
CI-1011	HR	0.63	0.56	0.46				
CI-1012	PDL	0.65	0.50	0.43				
CI-90	PDL	0.58	0.48	0.41				
CI-72d	PDL	0.59	0.47	0.43	HR	0.60	0.53	0.40
CI-89	HR	0.54	0.47	0.33	HR	0.54	0.47	0.40
CI-1014	PDL	0.59	0.48	0.42	PDL	0.57	0.44	0.41
CI-1013	PDL	0.63	0.50	0.42				
CI-67d	PDL+HR	0.57	0.52	0.47	HR+NL	0.61		
CI-1016	PDL	0.59	0.52	0.43				
CI-92					HR	0.56	0.51	0.40

As previously described, one of the potential points of improvement in the efficiency of a HF stimulation is to achieve the optimal Xf. Given the characteristics of the M1 layer, an effective HF is performed when the fracture does not grow beyond its boundaries, and all proppant penetrates extensionally in the reservoir to achieve the longest Xf. This will enable contact with the optimum SRV, increasing the contribution of hydrocarbon to the well and minimizing the additional expenses attributable to the proppant being pumped outside of the M1 productive interval.

To evaluate the efficiency of the HF performed in Campo Indio field, a non-radioactive tracer (NRT) proppant was pumped in two wells at the last stage of the HF. The NRT could be detected later by a pulsed neutron capture (PNC) log, enabling measurement of the HF growth.

Because the quality of a HF simulation depends on the mechanical properties of the formation, it is necessary to incorporate these characteristics in the simulator as input data. For these purposes, the geomechanical properties for the two analyzed wells were computed using the available openhole logs. A complete study, described in the following section, was available as reference for Campo Indio field geomechanical parameters.

Geomechanical Properties

A geomechanical model was built using correlation wells with full suite of sonic logs available in the area. The magnitude of the lithostatic stress gradient could be computed accurately through the integration of density logs for each well. At the Magallanes formation, the vertical stress (SV) is approximately 18.82 lb/gal (0.98 psi/ft) at 1440.0 mTVD.

Pore pressure measurements, performed with wireline formation testers, exhibit a normal gradient. Additional information obtained from DFIT and HF treatments also confirmed this behavior on the Magallanes formation pressure trend.

Because of the lack of measured acoustic shear travel time (DTS_Log) for some wells in the area, information from wells with an available full suite of sonic logs was used to build a multiregression model to predict a pseudo-acoustic shear travel time (DTS_MLR).

The multi-linear regression models enable a result curve to be predicted from several input curves, using a least squares regression routine, to determine the best fit to the input data.

The multi-linear regression model was built with information from 19 wells in the Campo Indio field. Input data for the model consisted of information of acoustic compressional (DTC), deep resistivity (RT), bulk density (RHOB), and neutron porosity (NPHI) logs, with which the best correlation coefficient obtained was R=0.88. The resultant equation for the computed pseudo DTS_MLR is:

$$DTS\_MLR = 10^{(-0.26016576 + 1.22286432 * Log(DTC) - 0.12915304 * Log(RT) + 0.39719764 * Log(RHOB) - 0.00943439 * Log(NPHI))}$$

Fig. 8 illustrates the correlation for the measured acoustic DTS_Log and the resultant DTS_MLR for the multiregression model for the 19 wells considered.

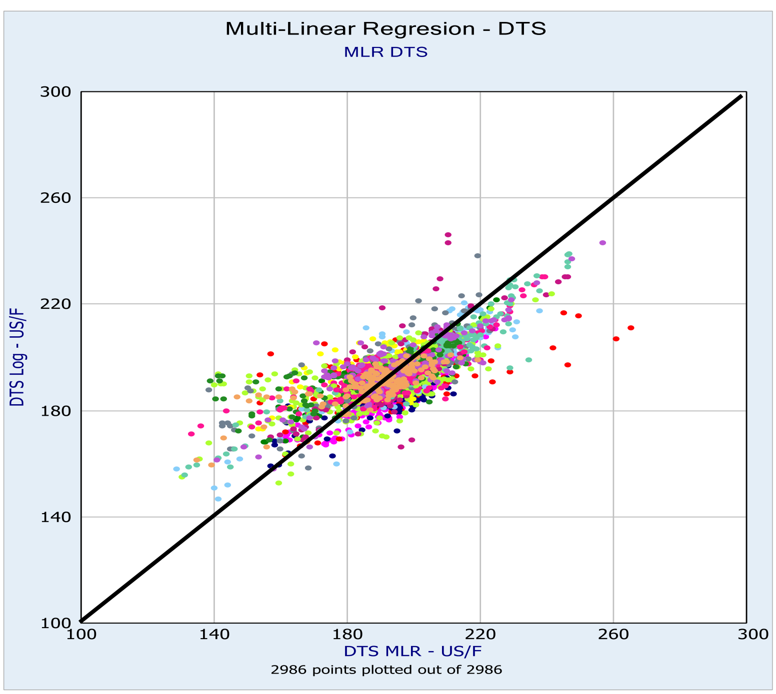

Fig. 8 – Correlation DTS_log vs. DTS_MLR.

The average unconfined compressive strength (UCS) for the Magallanes formation (top of M1) is approximately 3,045 psi. Poisson´s ratio is 0.25 with a coefficient of friction is 0.52; the brittleness value is 0.53, and Young´s modulus is 12,000,000 psi (Fig. 9).

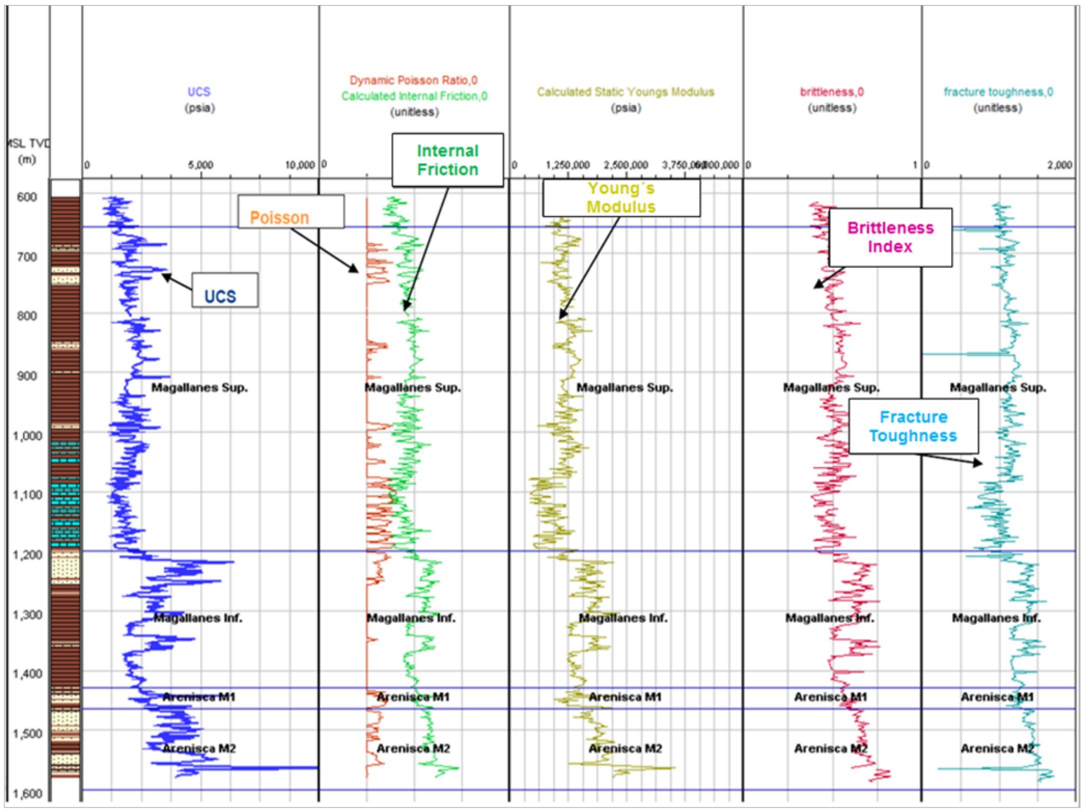

Fig. 9 – Mechanical properties for Well CI-50.

The minimum horizontal stress (Shmin) is 11.0 lb/gal (0.57 psi/ft), and the fracture gradient is 11.9 lb/gal at the top of Magallanes formation. The stress contrast is approximately 0.9 lb/gal. All of these reported geomechanical attributes were calibrated with the pressure integrity test (PIT), leakoff test (LOT), step-down rate tests (SDRT), DFIT, and minifrac tests available, and with information from HF operations (Fig. 10).

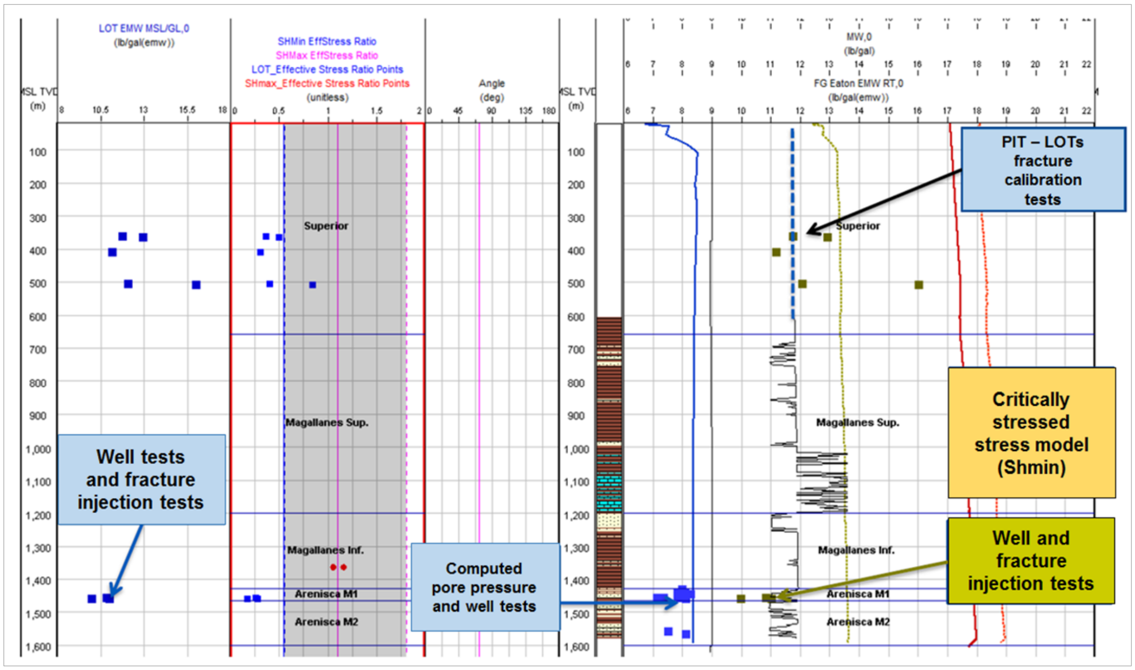

Fig. 10 – Shmin for Well CI-50.

The magnitude of the maximum horizontal stress (SHmax), determined by the stress polygon method, is approximately 19.37 lb/gal at the top of the M1 layer (Fig. 11). The most probable azimuth of the SHmax in the entire area of Campo Indio and Campo Indio east fields is approximately 72º, and it was estimated with an acoustic image log of Well CI-50, shown in Fig. 12. The direction of the SHmax is consistent with the regional trend observed in the world stress map (Fig. 13).

Fig. 11 shows the analysis of the stress polygon for Magallanes Lower formation.

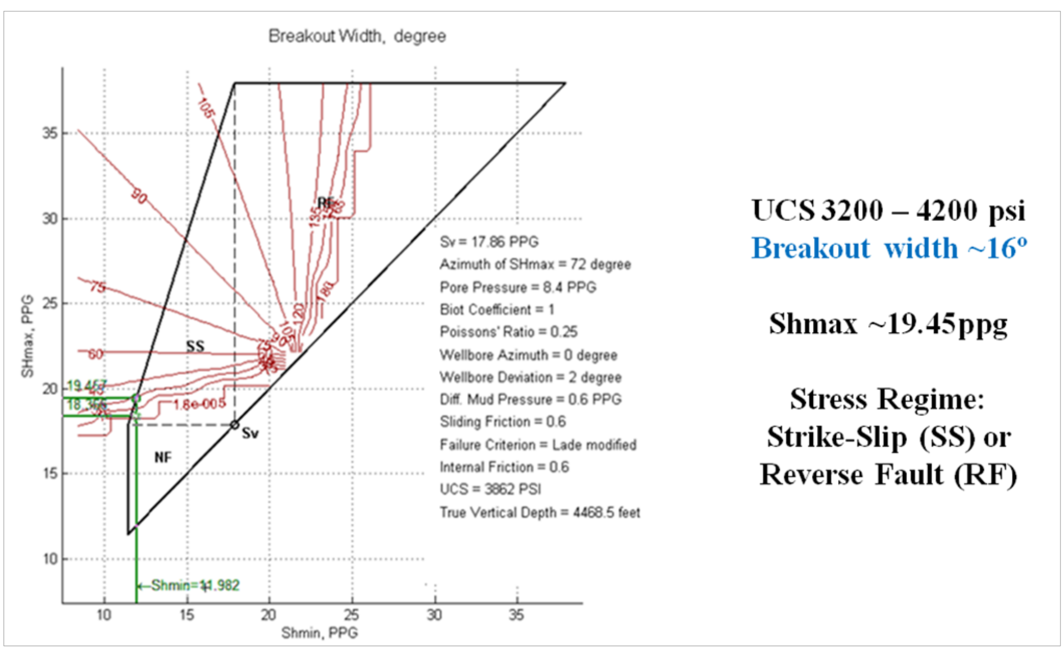

Fig. 11 – SHmax determination for Magallanes Lower formation.

The image log shown in Fig. 12 illustrates the acoustic image for Well CI-50 for the interval between 1269.9 and 1595.0 mMD. The maximum deviation for this well is approximately 2º. Some breakouts can be clearly identified on the image, with their of aperture 17º ± 3º and an orientation of 162º ± 14º. Based on these considerations, the orientation of the SHmax is determined on 72º ± 14º direction.

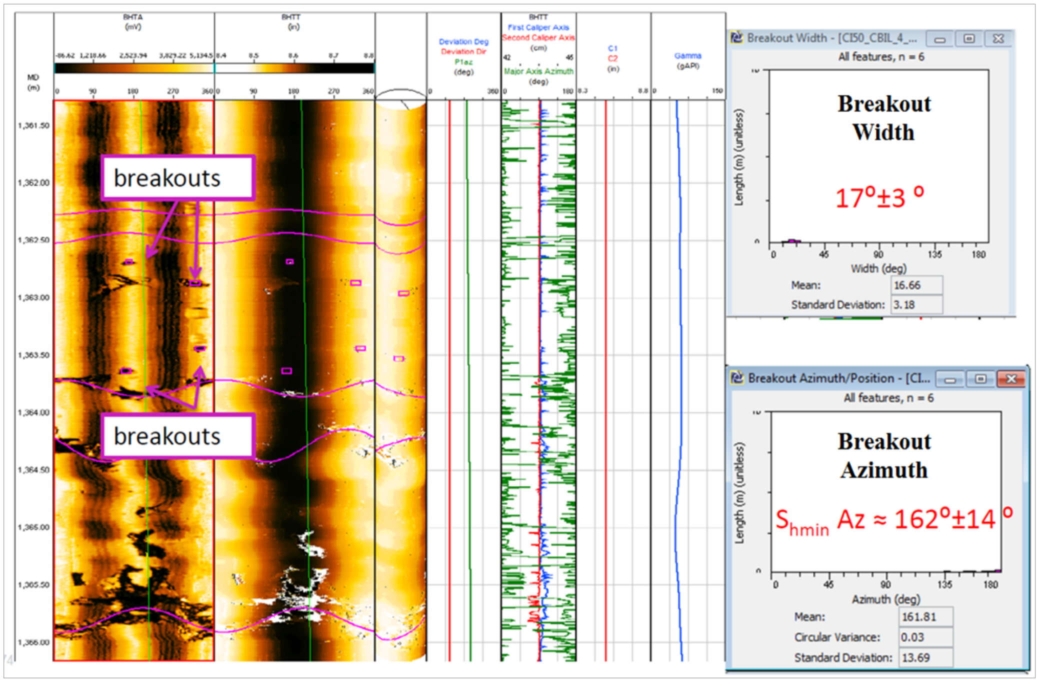

Fig. 12 – Breakouts observed in the interval between 1361.0 and 1366.5 mMD for Well CI-50.

The stress regime for the area is of a strike-slip type (Shmin< SV < SHmax). The induced HF is vertical and at 20 to 35º with respect to fault direction. Fig. 13 provides publicly available information of the stress regime predominant for the area of study and its orientation.

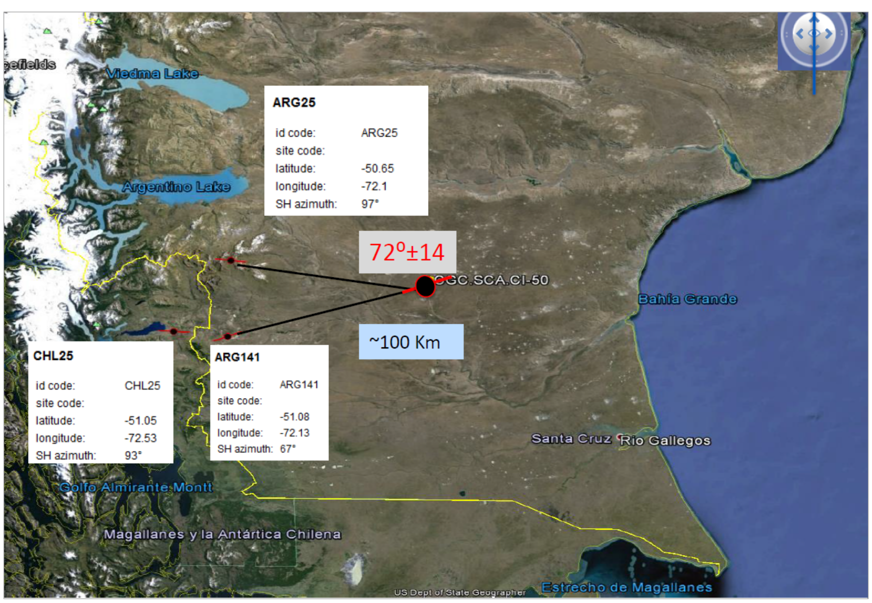

Fig. 13 – World stress map for Campo Indio, south of Santa Cruz Province (World Stress Map 2017).

Hydraulic Fracture Design – Assessed Wells

Two wells were selected for the HF vertical growth assessment in Campo Indio field, using NRT in both wells. The use of a PNC tool made it possible to identify the vertical growth of the fracture and to compare it with the initial HF design; this process also enabled a pressure match comparison obtained from the fracture simulator.

Wells Information

The wells selected for HF height assessment include Well CI-69(d) and Well CI-88. Table 2 and Table 3 provide depth references and reservoir properties information used for the assessments.

Table 2 – Depths of Reference

Well	CI-69(d)	CI-88
MD (m)	1570	1550
TVD (m)	1523	1550
Formation top (m)	1463	1415
Formation bottom (m)	1490	1445
Perforations MD top (m)	1474	1428
Perforations MD bottom (m)	1476	1431
Perforations TVD top (m)	1427	1428
Perforations TVD bottom (m)	1429	1431

Table 3 – Formation Properties

Parameters	CI-69(d)	CI-88
Closure pressure (psi)	2487	2330
Closure pressure gradient (psi/ft)	0.53	0.50
Pore pressure (psi)	1930	1670
Pore pressure gradient (psi/ft)	0.41	0.36
Porosity (%)	5 – 15	5 – 15
Temperature (°F)	160	157

The M1 layer was assessed for both wells; the depths corresponding to the fracture stimulations objective are very similar, and the mechanical properties characteristics are those expected for the area. Based on data previously obtained in field operations, the expected permeability ranges from 0.1 to 1.0 mD.

Pumping Schedules

Table 4 shows the pumping schedule for Well CI-69(d), and Table 5 provides information about the proppant and fluid volume.

Table 4 - Hydraulic Simulation Treatment - Well CI-69(d)											
Stage	Fluid System	Mesh	Rate	Volume	Concentration		Proppant			Cumulative	Accumulated Fluid
		#	bpm	gal	ppg	ppg	Type		Sacks	Sacks	gal
Minifrac	Linear gel	20	18.0	3000.0							3000.0
Registration Stops											
Treatment											
PrePad	Linear gel	20	4.0	2000.0							5000.0
PrePad	Linear gel	20	8.0	2000.0							7000.0
Pad	XL gel	25	12.0	2000.0					0.0	0.0	9000.0
Pad	XL gel	25	18.0	15000.0	0.50	0.50	Mesh 100		75.0	75.0	24000.0
Pad	XL gel	25	18.0	4000.0					0.0	75.0	28000.0
Proppant	XL gel	25	18.0	3000.0	1.00	1.00	Sand 20/40		30.0	105.0	31000.0
Proppant	XL gel	25	18.0	3000.0	2.00	2.00	Sand 20/40		60.0	165.0	34000.0
Proppant	XL gel	25	18.0	4000.0	3.00	3.00	Sand 20/40		120.0	285.0	38000.0
Proppant	XL gel	25	18.0	10000.0	4.00	4.00	Sand 20/40		400.0	685.0	48000.0
Proppant	XL gel	25	18.0	10000.0	5.00	5.00	Sand 20/40		500.0	1185.0	58000.0
Proppant	XL gel	25	18.0	10700.0	6.00	6.00	Sand 20/40		642.0	1827.0	68700.0
Proppant	XL gel	25	18.0	6000.0	6.00	6.00	Sand 20/40	C.E.*	360.0	2187.0	74700.0
Proppant	XL gel	20	18.0	9000.0	6.00	8.00	NRT 20/40	C.E.*	630.0	2817.0	83700.0
Proppant	XL gel	20	18.0	6000.0	8.00	8.00	NRT 20/40	C.E.*	480.0	3297.0	89700.0
Displacement	Linear gel	20#	18.0	1176.0							90876.0
*C.E. - Conductivity enhancer											

Table 5 - Proppant and Fluid Volume: Well CI-69(d)					
Proppant	Sacks	%	System	gal	m^3
Mesh 100	75.0	2.0	Linear gel	8,176.0	31.0
Proppant 20/40	2112.0	64.0	Gel XL	82,700.0	313.0
Ceramic 20/40	1110.0	34.0			
Total	3297.0	100.0	Total	90,876.0	344.0

Table 6 shows the pumping schedule for Well CI-88; Table 7 provides information about the proppant and fluids volume.

Table 6 - Hydraulic Stimulation Treatment - Well CI-88											
Stage	Fluid System	Mesh	Rate	Volume	Concentration		Proppant		Cumulative		Accumulated Fluid
		#	bpm	gal	ppg	ppg	Type	Sacks	Sacks		gal
DFIT	Water		8.0	1680.0							1680.0
Registration Stops											
Minifrac	Linear gel	20	8.0	630.0							2310.0
Minifrac	Linear gel	20	12.0	630.0							2940.0
Minifrac	Linear gel	20	18.0	1500.0							4440.0
Sdrt*	Linear gel	20	16.0	200.0							4640.0
Sdrt*	Linear gel	20	14.0	200.0							4840.0
Sdrt*	Linear gel	20	12.0	200.0							5040.0
Sdrt*	Linear gel	20	9.0	200.0							5240.0
Registration Stops											
Treatment											
PrePad	Linear gel	25	4.0	1500.0							6740.0
PrePad	Linear gel	25	8.0	1500.0							8240.0
Pad	XL gel	25	12.0	2000.0							10240.0
Pad	XL gel	25	18.0	13000.0							23240.0
Proppant	XL gel	25	18.0	1500.0	1.0	1.0	Ceramic 20/40	15.0	15.0		24740.0
Proppant	XL gel	25	18.0	3000.0	2.0	2.0	Ceramic 20/40	60.0	75.0		27740.0
Proppant	XL gel	25	18.0	4000.0	3.0	3.0	Ceramic 20/40	120.0	195.0		31740.0
Proppant	XL gel	25	18.0	6000.0	4.0	4.0	Ceramic 20/40	240.0	435.0		37740.0
Proppant	XL gel	25	18.0	11000.0	4.0	6.0	Ceramic 20/40	550.0	985.0		48740.0
Proppant	XL gel	25	18.0	19000.0	6.0	6.0	Ceramic 20/40	1140.0	2125.0		67740.0
Proppant	XL gel	25	18.0	9700.0	6.0	6.0	Ceramic 20/40	582.0	2707.0		77440.0
Proppant	XL gel	25	18.0	4000.0	6.0	7.0	NRT 20/40	C.E.*	260.0	2967.0	81440.0
Proppant	XL gel	25	18.0	1500.0	7.0	8.0	NRT 20/40	C.E.*	113.0	3080.0	82940.0
Displacement	Linear gel	20	18.0	1141.0							84081.0
*C.E. - conductivity enhancer											

Table 7 – Proppant and Fluids Volume - Well CI-88					
Proppant	Sacks	%	System	gal	m^3
Ceramic 20/40	2,125	69	Linear gel	7,701	29
NRT 20/40	955	31	Gel XL	74,700	283
Total	3,080	100	Total	82,401	312

It could be assumed that the results of given HF treatments for wells in the same area with similar petrophysical properties should yield identical gas production rates over time. However, other factors can affect the assumption before performing the HF. The work of designing HF through many years has included different parameters to be considered. In general terms, increasing the amount of proppant will improve the values of areal concentration, conductivity, fracture length, and other variables of interest.

Fig. 14 shows the HF simulation profile for Well CI-69(d); Table 8 summarizes reservoir and fracture parameters results obtained from the HF simulation performed for Well CI-69(d).

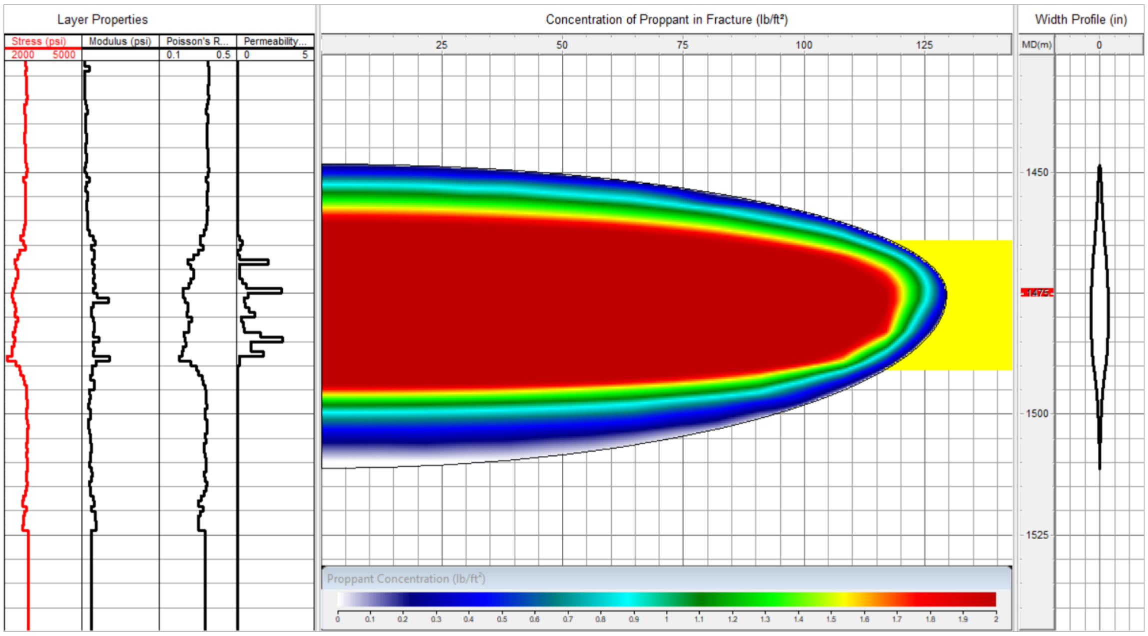

Fig. 14 – Fracture simulation for Well CI-69(d).

Table 8 – Reservoir and Fracture Parameters - Well CI-69(d)			
Reservoir	Design	Fracture	Design
Reservoir pressure	1930 psi	Fracture length	134.50 m
Reservoir pressure gradient	0.41 psi/ft	Proppant length	102.90 m
Total compressibility	1.39E-4 1/psi	Total fracture height	65.32 m
Viscosity	0.016 cp	Total proppant height	49.89 m
Permeability	0.01 – 0.10 mD	Average fracture width	0.292 in
Average porosity	20.0%	Proppant concentration	2.346 lb/ft^2
Closure stress pressure	2420 psi	Average fracture conductivity	2144 mD.ft
Closure stress gradient	0.516 psi/ft	Dimensionless fracture conductivity (FCD) ratio	8.6

Fig. 15 shows the HF simulation profile for Well CI-88.

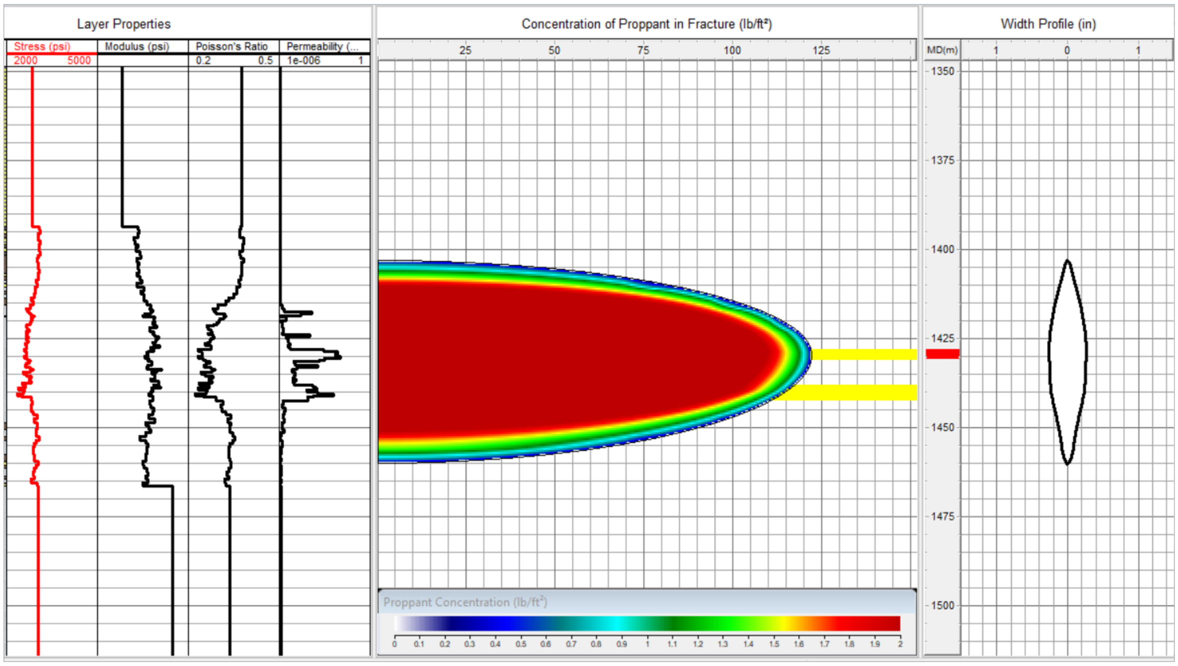

Fig. 15 – Fracture simulation Well CI-88.

Table 9 summarizes reservoir and fracture parameters results obtained from the HF simulation performed for Well CI-88.

Table 9 - Reservoir and Fracture Parameters - Well CI-88			
Reservoir	Design	Fracture	Design
Reservoir pressure	1,650 psi	Fracture length	122.60 m
Reservoir pressure gradient	0.35 psi/ft	Proppant length	108.50 m
Total compressibility	2.60E-4 1/psi	Total fracture height	57.21 m
Viscosity	0.030 cp	Total proppant height	50.63 m
Permeability	0.01 – 0.10 mD	Average fracture width	0.305 in
Average porosity	20.0%	Proppant concentration	2.623 lb/ft^2
Closure stress pressure	2575 psi	Average fracture conductivity	6630 mD.ft
Closure stress gradient	0.55 psi/ft	FCD ratio	39.84

Methodology for Fracture Height Assessment

To evaluate the growth in the HF height, a NRT was pumped during the last stage of the hydraulic fracture. A PNC log will be used later to detect the NRT location.

As previously introduced by Saldungaray et al. (2012) and more recently discussed by de Oliveira Neto and Yakovlev (2018), proppant containing or incorporating a high thermal neutron capture compound (HTNCC) has been used to measure the proppant location after placement, thus estimating fracture height along a vertical wellbore. The proppant is detected using standard pulsed neutron capture tools or compensated neutron tools, with detection resulting from the high thermal neutron absorptive properties of the tagged proppant.

The objective of this analysis was to estimate the HF height detected by NRT tagged proppant run before and after HF treatments. The physical principle of measurement of the PNC tool is based on the bombardment of the surrounding area of the well by high energy neutrons that emit the non-radioactive source of the tool; its decay is then monitored over time as a result of dispersion and capture. The dispersion and capture of neutrons depend on the constituent lithology of the rock, hydrogen, chlorine, and any external element that is in the formation, such as the NRT.

One of the most important decay parameters is the capture cross-section, also known as Sigma, which represents the macroscopic cross-section for the absorption of thermal neutrons of a volume of matter; it is measured in capture units (c.u.). The Sigma is the principal output of a PNC log.

One of the primary components of the NRT is gadolinium (Gd); this element, found in nature, has the largest capture cross-section or Sigma.

The PNC log was run before and after the HF to determine the presence of the NRT in the formation by comparing the difference in the recorded Sigma values. An increase in Sigma values after the HF means that the element in the formation has a greater capacity to stop the neutrons or a greater capture cross-section, which is related to the presence of NRT in the formation.

Fracture Height Assessment Well CI-69(d)

In Well CI-69(d), the HF treatment used 3,300 sacks of 20/40 sand and NRT 20/40 low density ceramic. The NRT determination was performed by running a PNC tool before and after the HF was made. As shown in Fig. 16, the Sigma value increases where the NRT is located (track SIGMA_Pre-Post). The difference between Sigma readings of PNC logs recorded before and after the HF treatment are shown in the SIGMA_Diff track. The HF height determined by the presence of the NRT comprises the interval from approximately 1470.0 to 1502.0 mMD.

The fracture was observed to have preferentially grown downward from the perforated interval (1474.0 to 1476.0 mMD), extending approximately 12 m below the lower limit of the M1. No clear fracture barriers are observed in the upper zone where the fracture stopped growing at 1470.0 mMD. The Shmin indicates a stress contrast of 400 psi for the M1 layer.

An increase of sigma borehole fluid (SIBH) is observed (Track SIGMA_BH) in intervals 1473.0 to 1478.0 mMD and 1484.0 to 1489.5 mMD. The SIBH is a shallow measurement that indicates the Sigma of the fluid or material that is immediately behind the pipe. Therefore, the increase of SIBH is most likely the result of the decanting of the NRT behind the casing after the HF treatment. The most noticeable increment of SIBH after the HF (SIBH_postF) is located in the interval between 1484.0 to 1489.5 mMD where no perforations exist. At the same interval, however, the cement has an irregular quality, which possibly enabled the decanting of the NRT behind the casing.

The observed decrease of Poisson´s ratio (PRSTA) and increase of Young's modulus (ESTA) indicates a more brittle interval (Track YM-PR). Similarly, the pseudo brittleness BRIT (Track PseudoBrit) computed indicates that the interval of greatest fragility extends from 1465.0 to 1490.0 mMD.

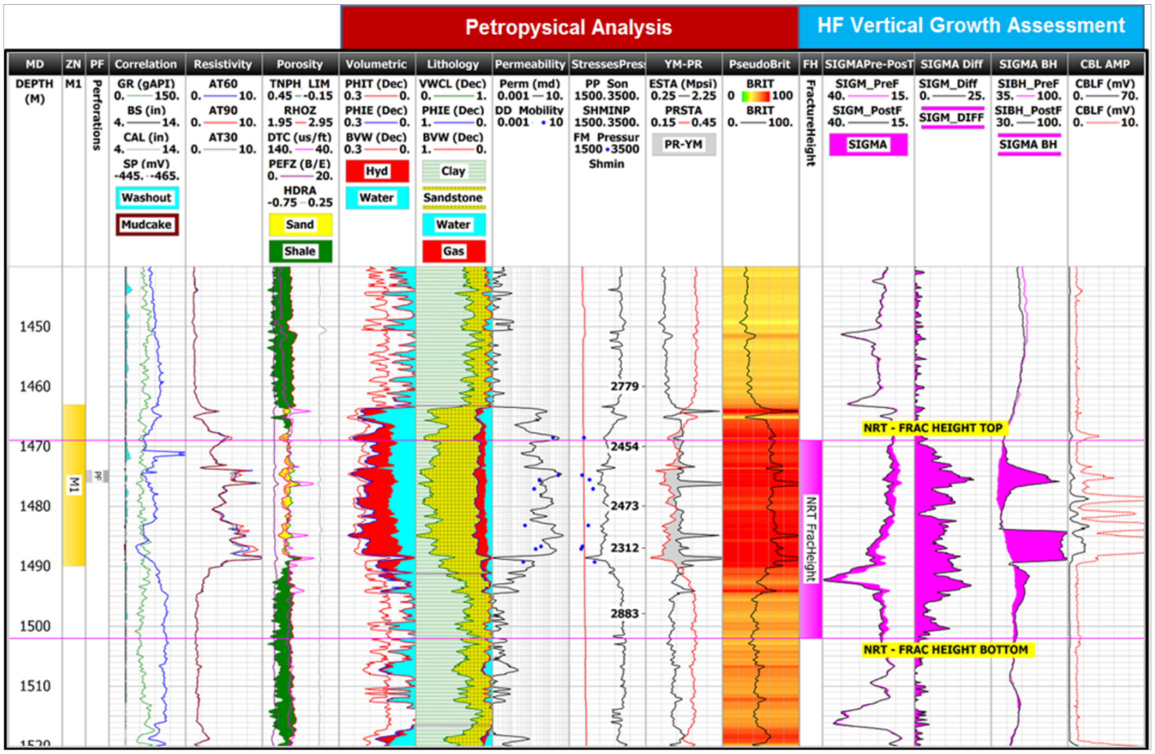

Fig. 16 – Fracture height assessment composite log – Well CI-69(d).

Table 10 summarizes the intervals previously defined.

Table 10 - HF Stimulation Treatment - Well CI-69(d)					
M1 Gross Interval (mMD)		Perforated Interval (mMD)		Interval w/NRT (mMD)	
1463.5	1492.5	1474.0	1476.0	1470.0	1502.0

Changes in the readings observed on the PNC logs run before and after an HF treatment depend on several factors; the most important of these factors include the concentration of the marker in the formation and the width of the fracture.

Smith et al. (2013) propose a method to quantify the width of the fracture as a function of the percentage increase of formation Sigma measured before and after the HF. Fig. 17 shows the quantification of the width of the fracture as a function of the change in Sigma.

The average change detected in Sigma values for the interval with NRT, is equal to 9% (DeltaSigma (%) = (SIGM_postF - SIGM_preF) / SIGM_preF).

From graph shown in Fig. 17 and the analysis of the percentage of incremental variation of Sigma values measured before and after the fracture, it can be inferred that the fracture has a width of 0.5 cm.

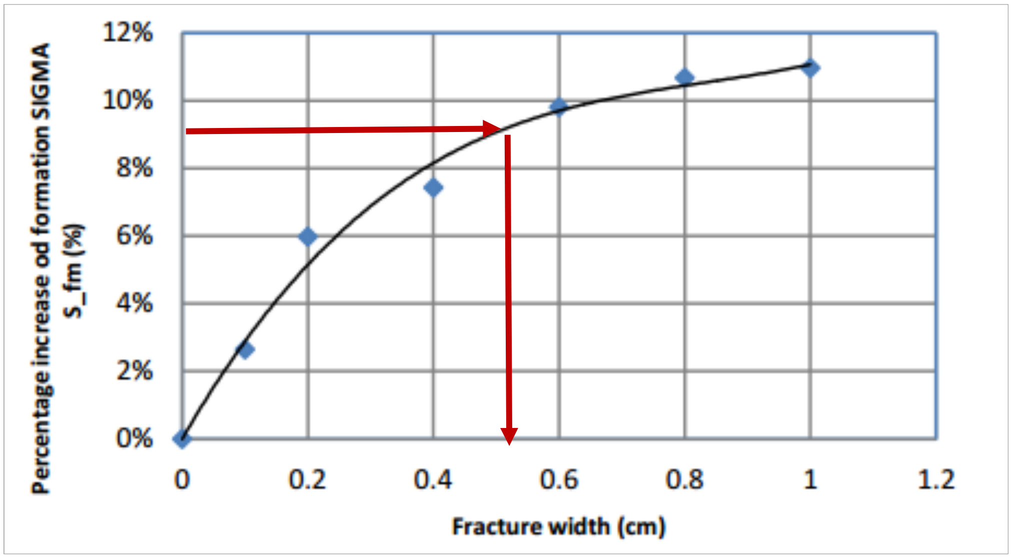

Fig. 17 – Percentage increase of Sigma formation vs. fracture width.

Fracture pressure matching was then performed in the simulator, obtaining the following results (Fig. 18):

- Reservoir pressure: 1,930 psi
- Closure stress pressure: 2,496 psi
- Fracture pressure gradient: 0.533 psi/ft

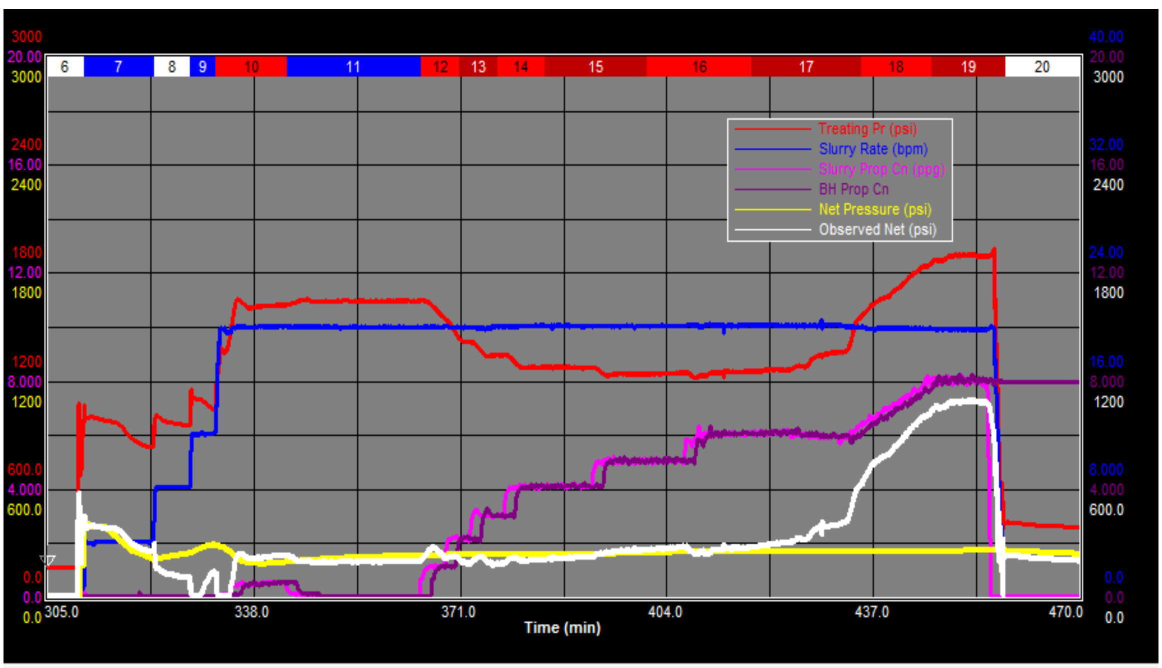

Fig. 18 – Fracture simulator net pressure matching.

Fig. 19 shows the fracture geometry matching; Table 11 summarizes the results of the HF geometry matching obtained in the simulator.

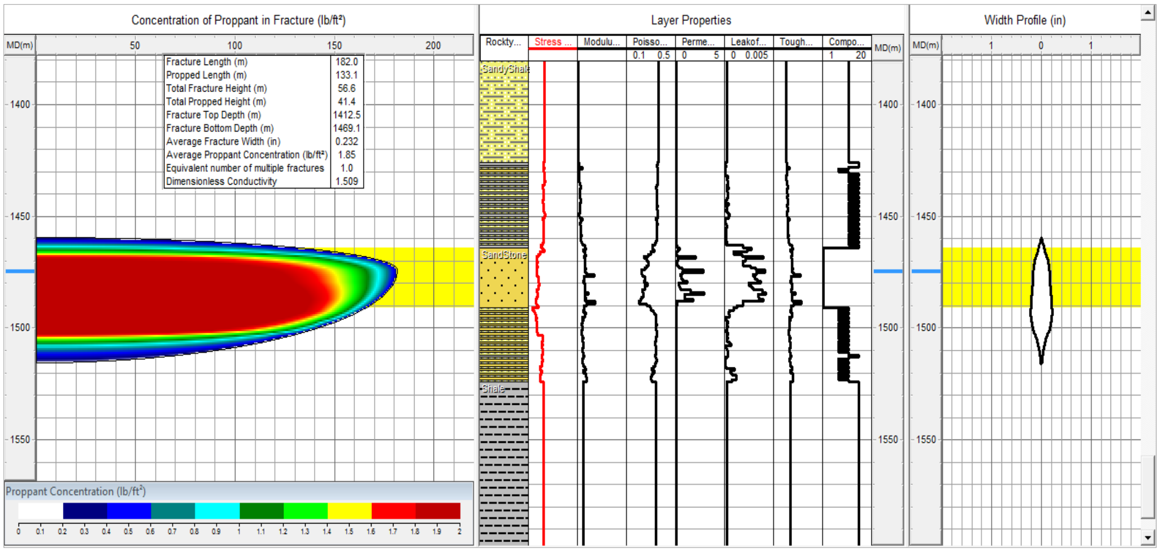

Fig. 19 – Fracture geometry matching.

Table 11 - HF Stimulation Treatment Matching - Well CI-69(d)							
M1 Gross Interval (mMD)		Perforated Interval (mMD)		Interval w/NRT (mMD)		HF Simulator Matching (mMD)	
1463.5	1492.5	1474.0	1476.0	1470.0	1502.0	1469.0	1504.0

The type of formation closure observed was HR; six multiple fractures were developed in the minifrac. The net pressure matching in the fracture simulator was finally achieved modelling three multiple fractures.

Fracture Height Assessment of Well CI-88

Continuing with the development of the Campo Indio field, Well CI-88 was drilled. The HF treatment performed used 3,050 sacks of 20/40 mesh proppant and NRT 20/40 low density ceramic.

The NRT was determined by running a PNC tool before and after the HF, as in the previous well. In this case, the PNC technology was run in high resolution spectroscopy mode to enable the detection and quantification of the fraction of Gd material present in the formation. This way, the Sigma along with the elementary capture spectroscopy information of both PNC runs were used to determine the changes produced by the presence of the NRT proppant in the formation.

Fig. 20 shows that there is a clear increment of Sigma values post fracture (SIGM_PostF - Track SIGMA Pre-Post) in the interval between 1418.7 and 1436.7 mMD as a result of the presence of NRT proppant. As shown in the figure, the HF was contained in the central part of the M1 layer, which includes the best reservoir quality and homogeneity.

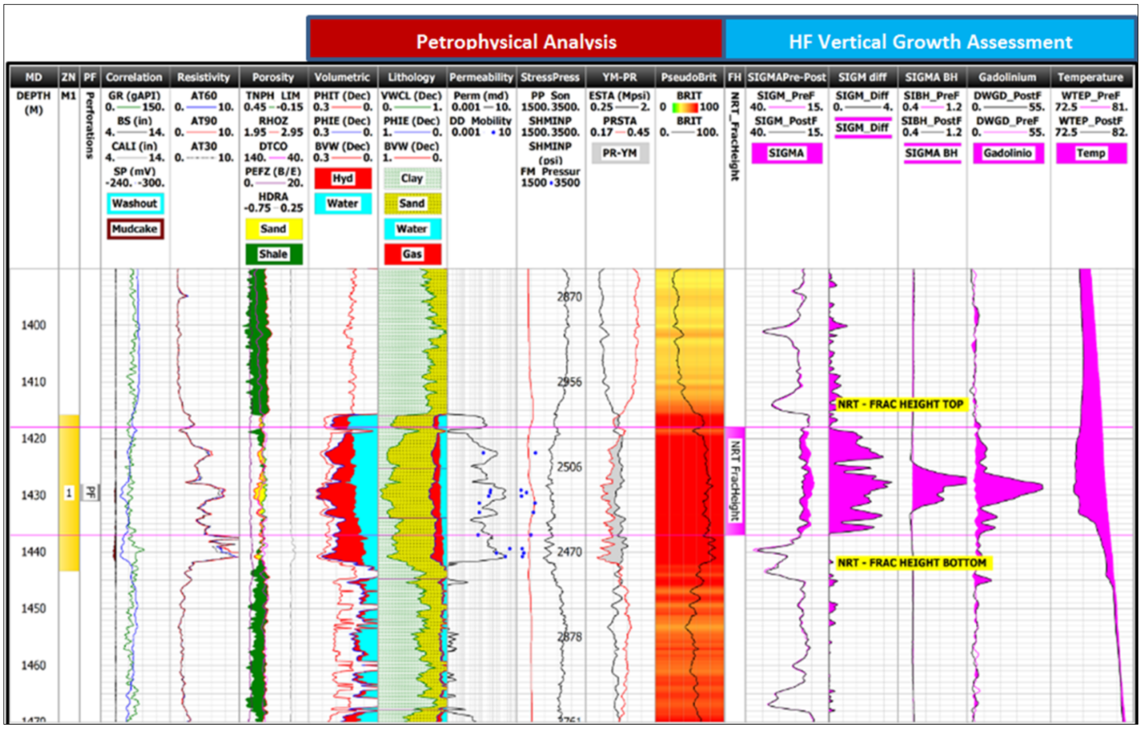

Fig. 20 – Fracture height assessment composite log – CI-88 well.

The elemental spectroscopy information obtained from the PNC run after the HF shows an increase in the Gd fraction, which clearly extends from 1416.0 to 1437.0 mMD (Track Gadolinium). Below 1437.0 mMD, the Gd fraction clearly decreases, showing that the HF has proppant up to 1446.0 mMD. It can be concluded that the height of the effective propped fracture would be between 1418.7 and 1436.7 mMD, whereas the HF not necessarily propped extends a little lower, perhaps up to 1446.0 mMD.

The temperature log run before and after the HF (Track Temperature) shows a cooling down effect caused by cooler fluid pumped into the formation during the HF between approximately 1446.0 and 1415.0 mMD.

The most remarkable increment of SIBH_PostF is evident in front of the perforated interval where the proppant appears to have found the preferred path in the way into the formation (Track SIGMA_BH).

Unlike Well CI-69(d) well, shallow PNC log readings do not indicate the presence of NRT behind the casing beyond the perforated interval; consequently, this could indicate that the quality of the cement was good before and maintained its integrity during the HF treatment. There is no cement log available to evaluate its quality.

A clayey intercalation is indicated in the upper part of the M1 where the fracture stops growing at 1418.0 mMD.

The Shmin pressure (Track StressPress) indicates a stress contrast of 450 psi at the top and 400 psi at the bottom, with respect to the recorded average for M1 interval.

The decrease of PRSTA and the increase of ESTA observed indicates a more brittle interval (Track YM-PR). Similarly, the pseudo brittleness BRIT (Track PseudoBrit) computed indicates that the interval of greatest fragility extends from 1415.0 to 1445.0 mMD.

Table 12 summarizes the previously defined intervals.

Table 12 - HF Stimulation Treatment - Well CI-88					
M1 Gross Interval (mMD)		Perforated Interval (mMD)		Interval w/NRT (mMD)	
1416.0	1445.0	1428.0	1431.0	1418.7	1436.7

Afterward, fracture pressure matching was performed on the simulator, as shown in Fig. 21; Fig. 22 shows the fracture geometry matching.

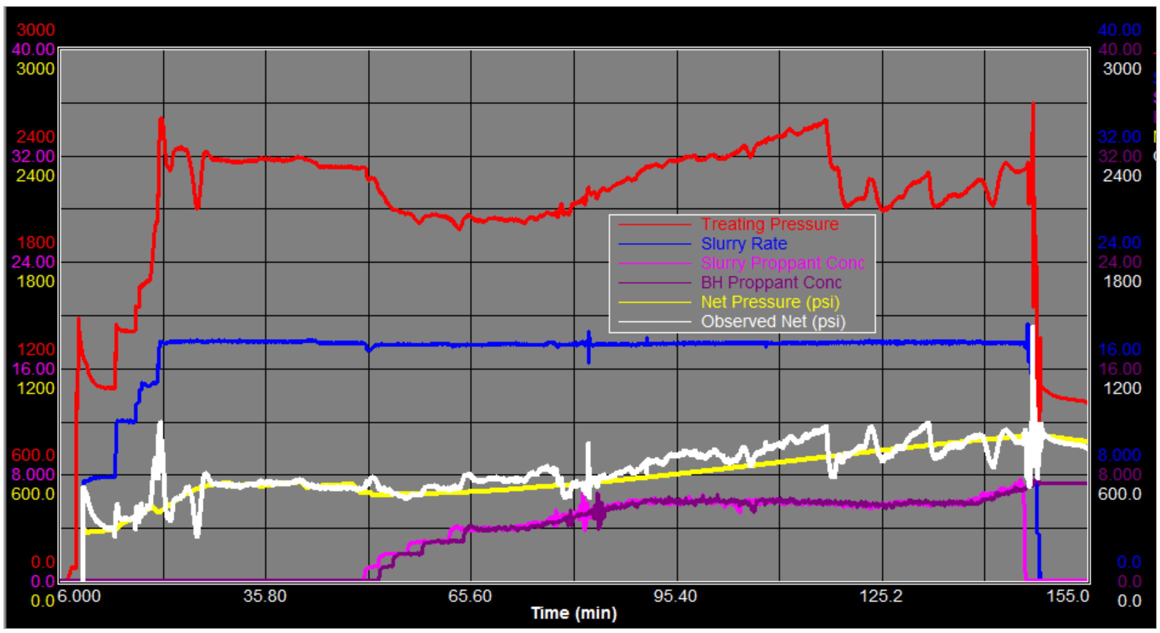

Fig. 21 – Fracture simulator net pressure matching.

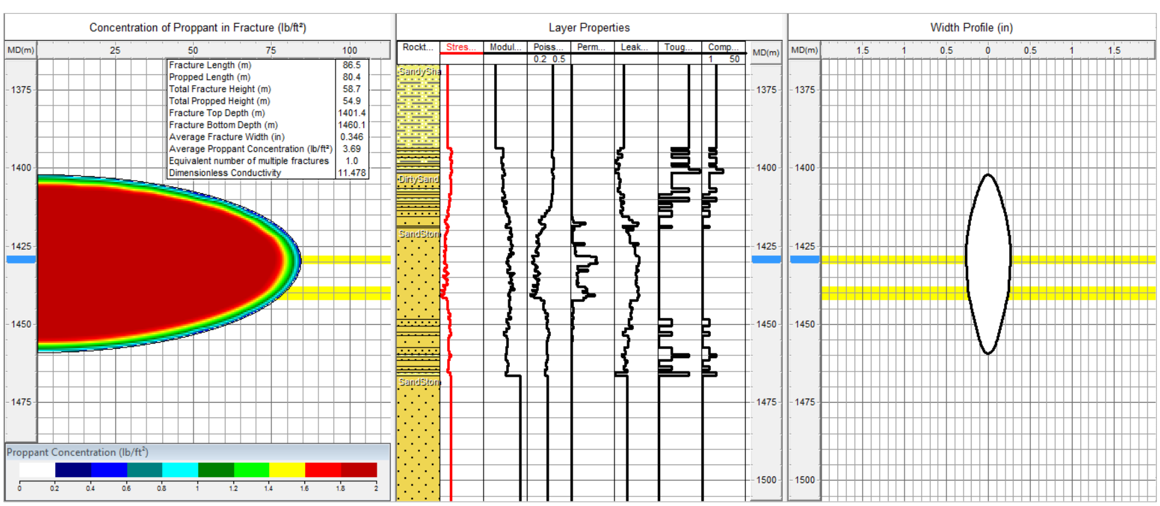

Fig. 22 – Fracture geometry matching.

Table 13 summarizes the results of the HF geometry matching obtained in the simulator.

Table 13 - HF Stimulation Treatment Matching Well CI-88							
M1 Gross Interval (mMD)		Perforated Interval (mMD)		Interval w/NRT (mMD)		HF Simulator Matching (mMD)	
1416.0	1445.0	1428.0	1431.0	1418.7	1436.7	1406.0	1456.0

The type of formation closure observed was HR. Four multiple fractures were developed in the DFIT, and three were developed in the minifrac. The net pressure matching in the fracture simulator was finally achieved modelling three multiple fractures.

As a summary of the HF treatments performed in both wells, Table 14 lists the main parameters and variation of the fracture gradient obtained. These differences, observed before and after HF treatments, explain the differences in the final geometry in accordance the results of the fracture height growth assessed through the detection of the pumped NRT proppant by the PNC tool.

Table 14 - Pre- and Post-HF Treatment Parameters Comparison - Wells CI-69(d) and CI-88								
Well	Rate (bpm)	Proppant (sacks)	ISIP Prefrac (psi)	Initial Fracture Gradient (psi/ft)	ISIP Post-frac (psi)	Final Fracture Gradient (psi/ft)	ISIP Variation (psi)	ISIP Variation (%)
CI-69(d)	20	3,303	660	0.58	415	0.52	-245	-37%
CI-88	18	3,044	590	0.56	1,095	0.67	505	86%

Conclusions

- The clayey intercalations observed in the lower part of the M1 layer of Well CI-88 between 1433.0 to 1440.0 mMD contributed to the containment of the fracture growth.
- The difference in the ISIPs explains the observed results in terms of the extension of the vertical growth of each fracture, with the HF clearly more contained in Well CI-88.
- The use of a low density ceramic proppant, which provides better conductivity as compared to the sand type, contributed to the expected production.
- The cement quality condition is believed to be the cause of the difference observed between the vertical growths of both HF stimulations. Cement quality is unknown for Well CI-88 because no cement bond log was available, but it is concluded that it should have a better cement quality than that observed in Well CI-69(d).
- The results indicate that the properties of the formation, the use of the low density ceramic proppant, and the cement conditions affect the final geometry registered in the appropriate profiles. This conclusion is indicated by the variation observed in the ISIP before and after the HF.
- The cases described in this paper show that actions should be taken in hydraulic fracture designs to limit vertical growth and to improve the concentration of proppant near the perforations. Aspects to consider in these actions include the rock properties, proppant, and condition of the cement.

Acknowledgments

The authors would like to thank the management of CGC for the permission to present and publish this paper.

Nomenclature

CE	*Conductivity enhancer*
DFIT	*Diagnostic fluid injection test*
DTC	*Acoustic compressional travel time*
DTS_Log	*Measured acoustic shear travel time*
DTS_MLR	*Multi-linear regression acoustic shear travel time*
FCD	*Dimensionless fracture conductivity*
ESTA	*Young's modulus*
Gd	*Gadolinium*
HDS	*High shot density perforating guns*
HF	*Hydraulic fracture*
HR	*High recession*
HTNCC	*High thermal neutron capture compound*
ISIP	*Initial instantaneous shut-in pressure*
LOT	*Leakoff test*
MINIFRAC	*Mini-fracture*
NL	*Normal leakoff*
NPHI	*Neutron porosity*
NRT	*Non-radioactive tracer proppant*
PDL	*Pressure dependent leakoff*
PIT	*Pressure integrity test*
PNC	*Pulsed neutrons capture log*
PRSTA	*Poisson´s ratio*
RHOB	*Bulk density*
RT	*Deep resistivity*
SDRT	*Step down test*
SIBH	*Sigma borehole fluid*
Shmax	*Maximum horizontal stress*
Shmin	*Minimum horizontal stress*
SRV	*Stimulated reservoir volume*
SV	*Vertical stress*
UCS	*Uniaxial compressive strength*
Xf	*Conductive fracture length*

References

Aimar, E., Cevallos, M., Cangini, A., Mas Cattapan, F., Vega, V. et al. 2018. *"Extensión y desarrollo de los reservorios de baja permeabilidad del yacimiento Campo Indio, formación Magallanes (Maastrichtiano tardío – Daniano), cuenca austral Argentina"*. Presented at the 10th Hydrocarbons Exploration and Development Congress, Mendoza, Argentina, 5-9 November. IAPG.

de Oliveira Neto, J.M. and Yakovlev, A., 2018, "*The use of pre & post fracture stimulation logs to better integrate static petrophysical analysis with dynamic data from production logs",* Presented at the SPWLA 59th Annual Logging Symposium, London, UK, 2–6 June. SPWLA-2018-EEEE.

Saldungaray, P.M., Palisch, T.T., Duenckel, R., 2012, "*Novel traceable proppant enables propped frac height measurement while reducing the environmental impact*", Presented at the SPE/EAGE European Unconventional Resources Conference and Exhibition, Vienna, Austria, 20–22 March. SPE-151696-MS. https://doi.org/10.2118/151696-MS.

Smith, H.D., Duenckel, R., and Han, X., 2013, "*A new nuclear logging method to locate proppant placement in induced fracture",* Presented at the SPWLA 54th Annual Logging Symposium, New Orleans, Louisiana, USA, 23-26 June. SPWLA-QQQ.

Solanet, F. and Melendo, F., 2017, "*Economic optimization through the re-design of wells in a tight gas marginal field*", Presented at the 3rd Latin American and Caribbean Congress of Drilling, Completion, Repair and Well Service, Buenos Aires, Argentina, 25-28 September. IAPG.

World Stress Map, 2017, "*The world stress map project - a service for science and earth system management*", http://www.world-stress-map.org/ (accessed 9 July 2019).

About the Authors

Miguel Jardel holds a bachelors degree in industrial engineering from National University of Cuyo (UNC) in Mendoza Argentina. He began his oil and gas career working as a cementing and stimulation engineer at San Antonio International Company. For seven years, Jardel worked for various clients in the Golfo San Jorge and Austral basins. In 2014, he joined the production enhancement group at Halliburton where he worked on projects in the Chubut and Santa Cruz provinces in various formations of the Golfo San Jorge and Austral basins. Jardel currently works as an account leader for CGC and provides technical support for case studies in the Golfo San Jorge basin.

Santiago Casalá holds a bachelors degree in industrial engineering from National Technological University (UTN) in Buenos Aires, Argentina. He works as a petrophysicist and has more than 15 years of E&P experience. Casalá currently works at Halliburton with the Unconventional Reservoirs Solutions team, based in Buenos Aires, Argentina, as a petrophysical technical advisor. He began his career in 2000, working in a laboratory to perform conventional and special core analysis. In 2006, Casalá joined the Formation and Reservoir Solutions team in Argentina as log analyst. In 2011, he was transferred to the United Kingdom to join the Formation and Reservoir Solutions team in Aberdeen, Scotland as senior petrophysicist. In this assignment, Casalá worked on several North Sea intervention, surveillance, and exploratory projects.

Maria Florencia Melendo holds a bachelors degree in chemical engineering from the University of Buenos Aires (UBA) in Buenos Aires, Argentina, with a specialization in well completion from Buenos Aires Institute of Technology (ITBA). She is a well completion specialist in unconventional reservoirs. During her more than 10 years of experience in the oil and gas industry, Melendo has worked as a project manager and reservoir engineer at Petrobras Argentina and CGC. She currently works at CGC as a production engineer, specializing in fractures in the Austral basin.

Gustavo Kruse holds a bachelors degree in civil engineering from the National Technology University in Santa Fe, Argentina. He has 22 years of experience in the design and performance of cementing and stimulation operations for gas and oil wells in most of Argentina's productive basins, working for BJ Services and Halliburton Argentina. Kruse has also worked on sand control projects, water control, and other special services. He is currently a technical consultant on fracturing and cementation projects.